Electronic Supplementary Material (ESI) for RSC Advances.


# Supplemental Information for

# Two magnon scattering and anti-damping behavior in two-dimensional *epitaxial* TiN/Py($t_{Py}$)/$\beta$-Ta($t_{Ta}$) system

Nilamani Behera[a] Ankit Kumar[a,b] Sujeet Chaudhary[a*] and Dinesh K. Pandya[a]

[a]*Thin Film Laboratory, Department of Physics, Indian Institute of Technology Delhi, New Delhi 110016, India*

[b]*Department of Engineering Sciences, Box 516, Uppsala University, 751 21 Uppsala, Sweden*

**Following supporting data/information is supplied through this additional file:**

1. **RHEED analysis of *epitaxial* Si/TiN(8 nm)/Py (3, 5, and 10 nm)**
2. **Details of fitting parameters used in Fig. 3(b) and Fig. 3(d)**
3. **Comparison of geometrical factor "*S*" as obtained from $\Delta H$-vs.-$t_{Py}$ and $\Delta H$-vs.-$1/t_{Py}^2$ plot**
4. ***In-plane* $f$-vs.-$H_r$- and $\Delta H$-vs.-$f$ of *epitaxial* bilayers: Si/TiN(8 nm)/Py(12 nm)/ $\beta$-Ta(1.5, 4, 5, 7.5, 10.5 nm)**
5. **Thickness dependence of effective magnetization in Si/TiN(8 nm)/Py($t_{Py}$ nm) and Si/TiN(8 nm)/Py(12 nm)/$\beta$-Ta ($t_{Ta}$) bilayers**
6. **$1/t_{Py}$ dependence of effective damping $\alpha_{eff}(t_{Py})$ i.e. $\alpha_{eff}(t_{Py})$-vs.-$1/t_{Py}$ in Si/TiN(8 nm)/Py($t_{Py}$ nm) system**
7. **Surface topography (RMS roughness) studies in Si/TiN(8 nm)/Py($t_{Py}$ nm) and Si/TiN(8 nm)/Py(12 nm)/$\beta$-Ta ($t_{Ta}$) system by atomic force microscopy (AFM)**

These are briefly described in the following.

## 1. RHEED analysis of *epitaxial* Si/TiN(8 nm)/Py (3, 5, and 10 nm)

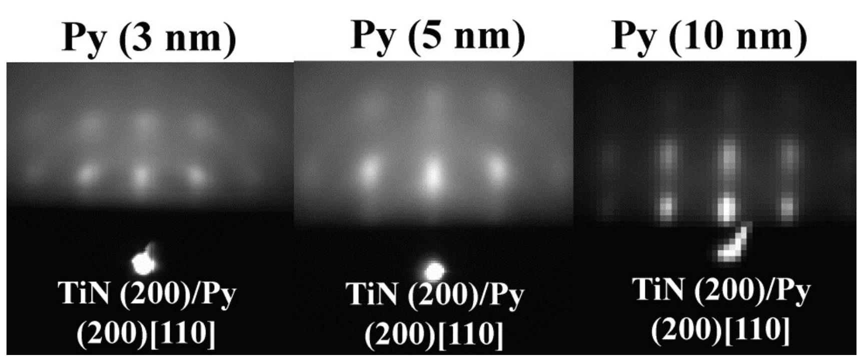

Fig. SI 1 RHEED patterns of Py 3 nm, 5 nm, and 10 nm samples grown on TiN(200) [001]. The epitaxial relationship between Py and the TiN buffer layer is TiN(200)//Py(200); Py[001]//TiN[001].

RHEED patterns clearly indicate that the growth of Py films of thickness less than 12 nm is 3D island type as compared to 2-D growth at higher thicknesses, already shown in Fig. 1 of MS.

**2. Details of fitting parameters used in Fig. 3(b) and Fig. 3(d)**

**I.** Table-1 presents the fitting parameters, the renormalization factor $r$ and $\frac{2K_S}{M_s}$, that are used to fit the data of Fig. 3(b) by using eqn (4) as thickness dependent shift of $H_r$. Here we have taken $4\pi M_s$ =1088 mT as it obtained from the fitting of $4\pi M_{eff}$-vs.-$t_{Py}$ for all bare Si/TiN(8 nm)/Py ($t_{Py}$=3-20 nm), i.e. bare *epi*-Py samples shown in Fig. SI 3(a).

**II.** Table-2 shows the list of fitting parameters that are used to fit the data in Fig. 3(d) by using the eqn (6) within the error of measurement, the value of geometrical factor "*S*" which arises from surface roughness and defects is almost of same order of magnitude as reported by Arias and Mills theory.[30] It can be seen that "*S*" varies in the range from 0.047 to 0.144 nm$^2$ for all the thicknesses of $t_{Py}$ at all the investigated frequencies (6-10 GHz), $\alpha$ remains constant within the error of measurement.

**Table-1: Fitting parameters obtained using eqn (4) for $H_r$-vs.-$t_{Py}$ data of Fig. 3(b).**

| *Fitting parameters* | *Frequency (GHz)* | | | | |
|---|---|---|---|---|---|
| | **6** | **7** | **8** | **9** | **10** |
| $r$ **(mT$^{-1}$)** | **-8.85(±.90)×10$^{-5}$** | **-1.27(±0.14)×10$^{-4}$** | **-1.65(±0.06)×10$^{-4}$** | **-1.88(±0.05)×10$^{-4}$** | **-2.16(±0.46)×10$^{-4}$** |
| $\frac{2K_S}{M_s}$ **(mT.nm)** | **-1.33(±0.30)×10$^3$** | **-1.53(±0.31)×10$^3$** | **-1.68(±0.34)×10$^3$** | **-1.65(±0.20)×10$^3$** | **-1.65(±0.21)×10$^3$** |

**Table-2: Fitting parameters obtained using Eq. (6) for $\Delta H$-vs.-$t_{Py}$ data of Fig. 3(d).**

| *Fitting parameters* | *Frequency (GHz)* | | | | |
|---|---|---|---|---|---|
| | **6** | **7** | **8** | **9** | **10** |
| $S$ **(nm$^2$)** | **0.100 (± 0.003) - 0.144(±0.005)** | **0.073(± 0.002)- 0.107(± 0.003)** | **0.048 (± 0.002)- 0.073 (± 0.003)** | **0.057(± 0.002)- 0.086 (± 0.003)** | **0.053 (±0.003)- 0.077 (± 0.004)** |
| $\alpha_{int.}$ | **0.0082 (±0.0002)** | **0.0083 (±0.0002)** | **0.0083(±0.0002)** | **0.0083 (±0.0002)** | **0.0083 (±0.0002)** |

**3. Comparison of geometrical factor "*S*" as obtained from $\Delta H$-vs.-$t_{Py}$ *and* $\Delta H$-vs.-$1/t_{Py}^2$ plot**

We have plotted the $1/t_{Py}^2$ dependence of $\Delta H$ i.e. $\Delta H$-vs.-$1/t_{Py}^2$ and solid lines are fitted with equation (6). The $\Delta H$-vs.-$1/t_{Py}^2$ dependency is compared with $\Delta H$-vs.-$t_{Py}$ dependency in Fig. SI2. In all the cases, the $S$ values are almost same with previous values within the error of measurement as determined by using eqn (6), (See Table 2). For further clarity, the calculated values of $S$ parameters as determined from the $\Delta H$-vs.-$t_{Py}$ fit and $\Delta H$-vs.-$1/t_{Py}^2$ are shown in Fig. SI3

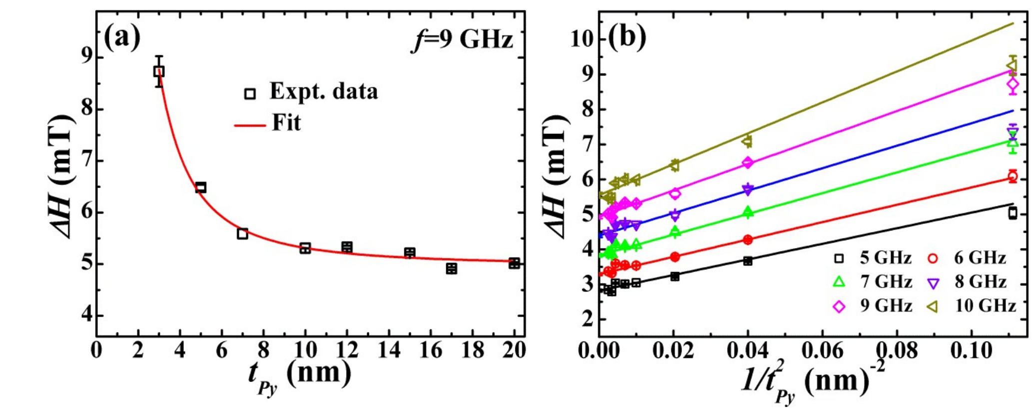


Fig. SI 2: (a) $\Delta H$-vs.-$t_{Py}$ at 9 GHz and (b) $\Delta H$-vs.-$1/t_{Py}^2$ at 5-10 GHz, for Si/TiN(8 nm)/Py($t_{Py}$=3-20 nm) multilayer thin films. Open symbols are experimental data and solid lines are fit to experimental data by using eqn (6).

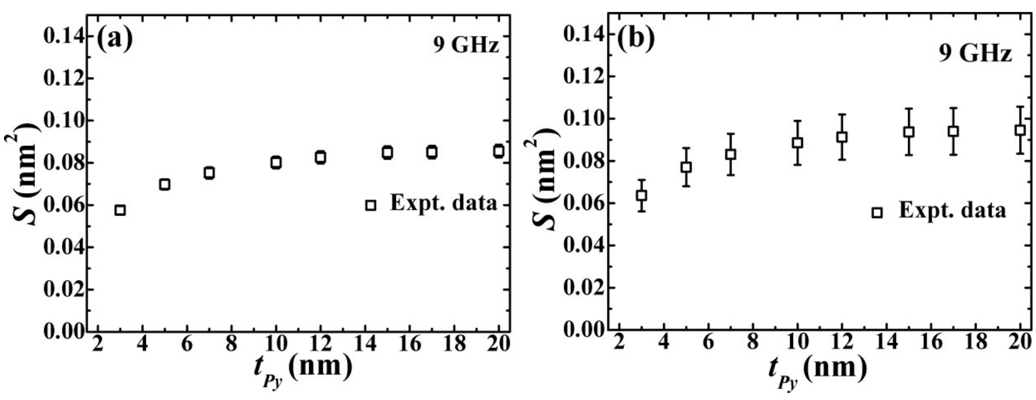


Fig. SI 3: $S$-vs.-$t_{Py}$ plots (a) calculated from $\Delta H$-vs.-$t_{Py}$ fit and (b) $\Delta H$-vs.-$1/t_{Py}^2$ for Si/TiN(8 nm)/Py($t_{Py}$=3-20 nm) multilayer thin films at 9 GHz. Open symbols are experimental data.

**4. *In-plane f*-vs.-$H_r$- and $\Delta H$-vs.-*f* of *epitaxial* bilayers: Si/TiN(8 nm)/Py(12 nm)/ β-Ta(1.5, 4, 5, 7.5, 10.5 nm)**

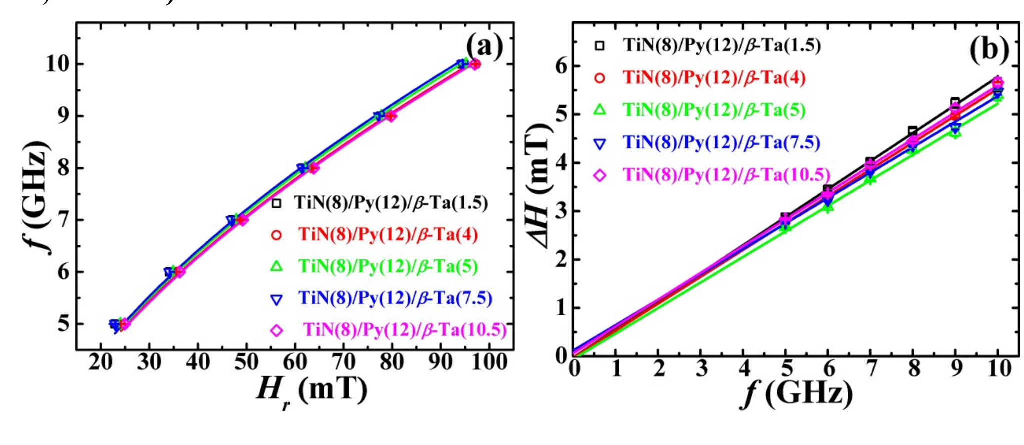

Fig. SI 4: (a) The *in-plane* resonance frequency $(f)$ vs. resonance field $(H_r)$ and (b) $\Delta H$-vs.-$f$ for samples with different $t_{Ta}$ and solid lines shows the fits employing eqn (2) and eqn (5) respectively.

**5. Thickness dependence of effective magnetization in Si/TiN(8 nm)/Py($t_{Py}$ nm) and Si/TiN(8 nm)/Py(12 nm)/β-Ta ($t_{Ta}$) bilayers**

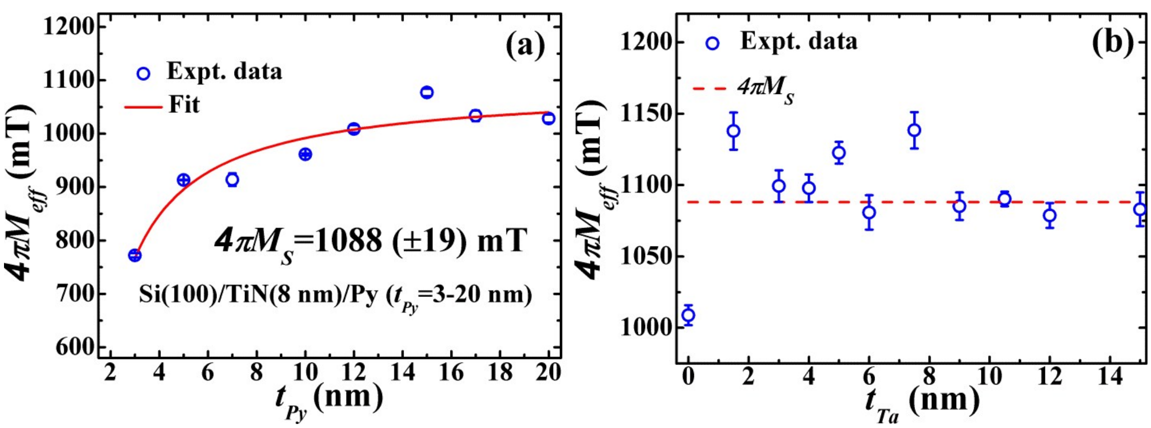


Fig. SI 5: Variation of effective magnetization, $4\pi M_{eff}$ in (a) Si/TiN(8 nm)/Py($t_{Py}$ nm), and (b) Si/TiN(8 nm)/Py(12 nm)/β-Ta ($t_{Ta}$).bilayers obtained from the fittings of eqn (2). Symbols are the experimental data within error of measurement and solid line is fit to data. Dashed line gives the $4\pi M_S$ value for *epi*-Py layer.

**6. $1/t_{Py}$ dependence of effective damping $\alpha_{eff}(t_{Py})$ i.e. $\alpha_{eff}(t_{Py})$-vs.-$1/t_{Py}$ in Si/TiN(8 nm)/Py($t_{Py}$ nm) system.**

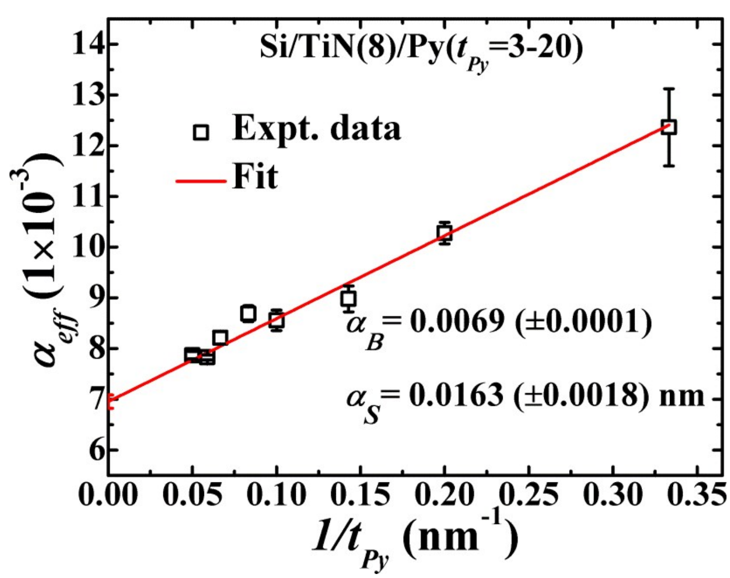

Fig. SI 6: $\alpha_{eff}(t_{Py})$-vs.-$1/t_{Py}$ plots for Si/TiN(8 nm)/Py($t_{Py}$=3-20 nm) Open symbols are experimental data and the solid line is linear fit to experimental data for extracting the bulk and surface contributions to the overall damping.

**7. Surface topography (RMS roughness) studies in Si/TiN(8 nm)/Py($t_{Py}$ nm) and Si/TiN(8 nm)/Py(12 nm)/*β*-Ta ($t_{Ta}$) system by atomic force microscopy (AFM)**

The estimated values of RMS roughness are 0.86 0.70 nm and 0.33 nm for Si/TiN(8)/Py(12)/Ta(1.5, 5, 6 nm) samples, and 1.22 nm, 0.44, and 0.69 nm for Si/TiN(8)/Py(7, 10, 12 nm) samples within the error of 1%, respectively as shown in Fig. SI 6.

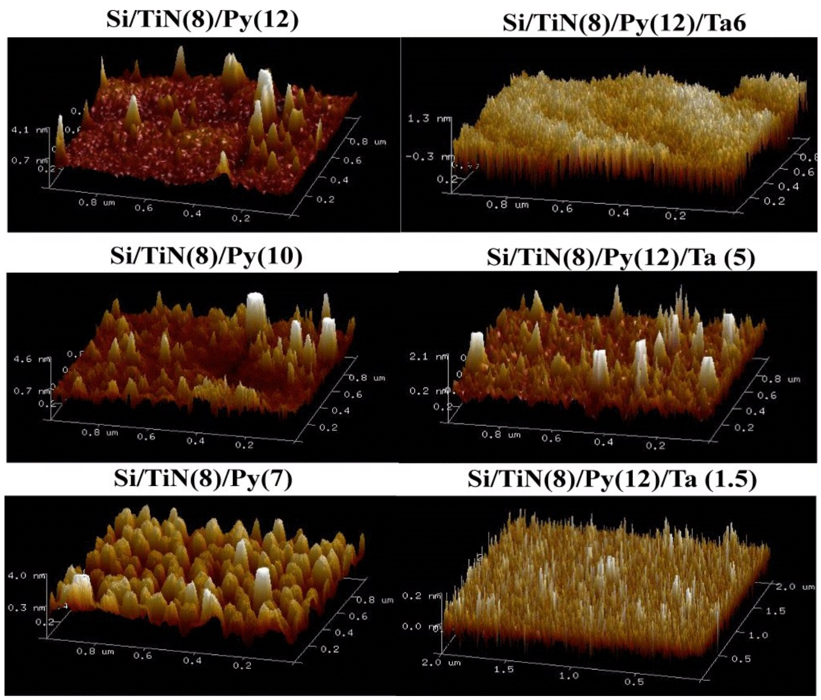


Fig. SI 7: Atomic force microscopy (AFM) images of Si/TiN(8 nm)/Py($t_{Py}$=7, 10, 12 nm) and Si/TiN(8 nm)/Py(12)/Ta($t_{Ta}$=1.5, 5, 6 nm) samples showing their surface topography.